LA-13507-MS

Stratigraphy and Geologic Structure at the SCC and NISC Building Sites, Technical Area 3, Los Alamos National Laboratory, New Mexico

Los Alamos
NATIONAL LABORATORY

Los Alamos National Laboratory is operated by the University of California for the United States Department of Energy under contract W-7405-ENG-36.

Prepared by Lanny Piotrowski, Group EES-1.

An Affirmative Action/Equal Opportunity Employer

LA-13507-MS

UC-903
Issued: September 1998

Stratigraphy and Geologic Structure at the SCC and NISC Building Sites, Technical Area 3, Los Alamos National Laboratory, New Mexico

*Donathon Krier**
*Florie Caporuscio***
*Alexis Lavine**
*Jamie Gardner**

**Earth and Environmental Sciences Division, Geology and Geochemistry Group, Los Alamos National Laboratory, Los Alamos, NM 87545.*
***Benchmark Environmental Inc., 117 Longview Dr., White Rock, NM 87544.*

Los Alamos
NATIONAL LABORATORY
Los Alamos, New Mexico 87545

STRATIGRAPHY AND GEOLOGIC STRUCTURE AT THE SCC AND NISC BUILDING SITES, TECHNICAL AREA 3, LOS ALAMOS NATIONAL LABORATORY, NEW MEXICO

by

Donathon Krier
Florie Caporuscio
Alexis Lavine
Jamie Gardner

ABSTRACT

Ten closely spaced, shallow (<100 ft) drill cores were obtained from the 1.22-Ma-old Bandelier Tuff at a 4-acre site for proposed construction at Los Alamos National Laboratory, New Mexico. The goal of the investigation was to identify faults that may have potential for earthquake-induced surface ruptures at the site. Careful mapping of contact surfaces within the Bandelier Tuff was supplemented with results of geochemical analyses to establish unit boundaries with a high degree of accuracy. Analysis shows that the upper contact surface of Unit 3 of the Bandelier Tuff provides no evidence of faults beneath the building site, and that the subsurface structure is consistent with a shallowly dipping (<2°), unbroken block. Because no significant or cumulative faulting events have disturbed the site in the last 1.22 million years, it is unlikely that surface rupture will occur at the site in future large earthquakes. Uncertainty analysis suggests that this method would detect faults with ≥2 ft of cumulative stratigraphic separation.

I. INTRODUCTION

Previous studies have shown that the major, potentially active faults that may affect Los Alamos National Laboratory (LANL) are the Pajarito, Rendija Canyon, and Guaje Mountain zones (Figure 1a) (Dransfield and Gardner, 1985; Gardner and House, 1987; Wong et al., 1995). These fault zones are commonly taken to constitute the Pajarito Fault System (e.g., Gardner and House, 1987), which defines the local active boundary of deformation of the Rio Grande Rift, a major tectonic feature of the North American continent (Gardner and Goff, 1984). How the faults of this system may physically connect or kinematically interact has important bearing on seismic hazards issues at Los Alamos and is the focus of on-going studies. The southern end of the Rendija Canyon fault was inferred to pass through or near Technical Area (TA)-55 by Wong et al., (1995); however, detailed work by Gardner et al. (1998) showed that the otherwise north-south trending fault does not pass through TA-55, but may, instead, pass through TA-3 as multiple southwest-trending splays. Additionally, aerial photo lineaments that may represent southwest-trending splays of the Rendija Canyon fault appear to converge on TA-3.

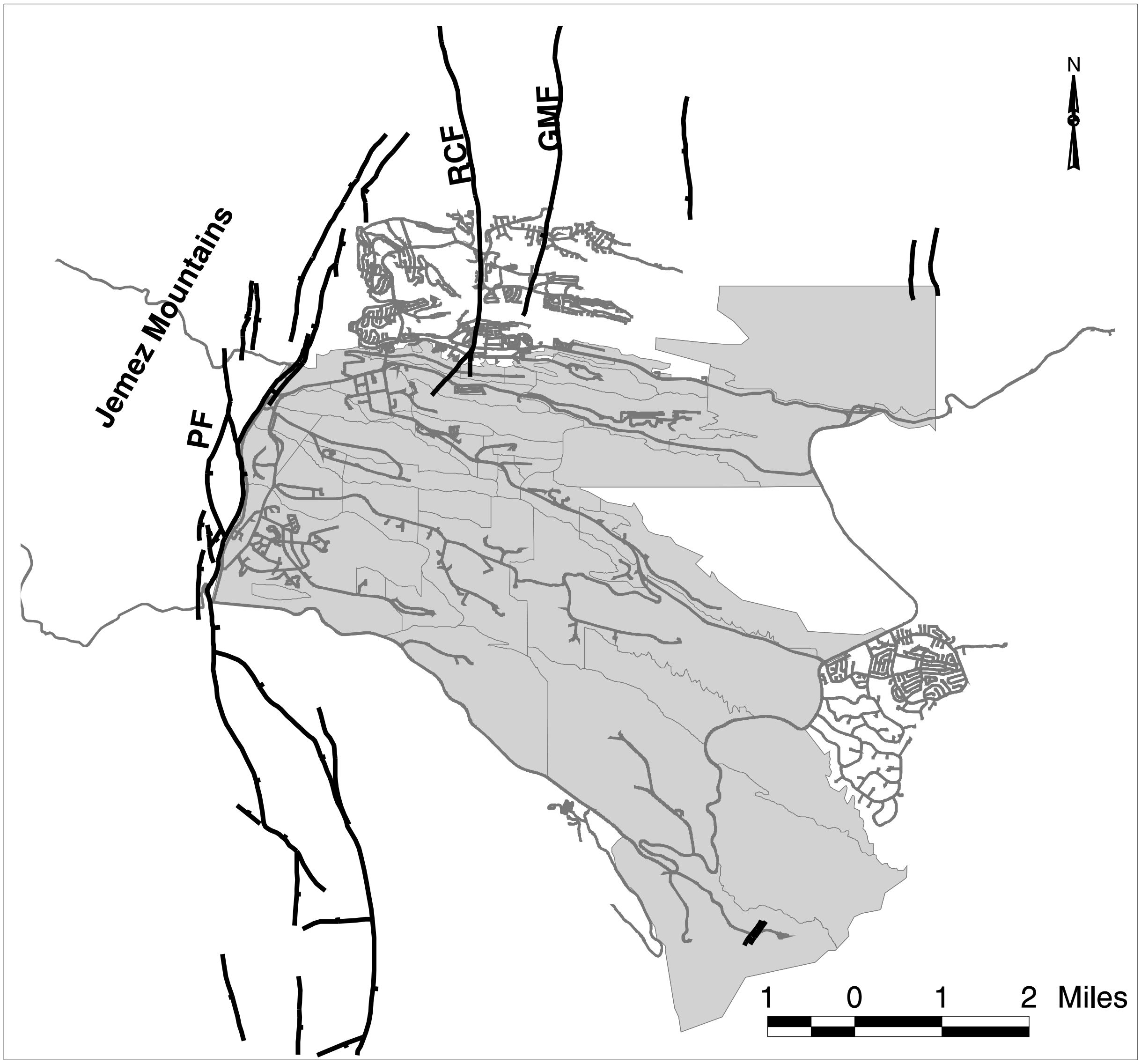

Figure 1a. Map showing the area of Los Alamos National Laboratory (shaded grey) and faults of the Pajarito Fault System (thick lines with bar on downthrown side): PF = Pajarito Fault, RCF = Rendija Canyon Fault, GMF = Guaje Mountain Fault.

As part of the Los Alamos National Laboratory Seismic Hazards Program, ten boreholes were drilled at the site of two proposed facilities in TA-3 to obtain information on the presence or absence of near-surface normal faults (Figure 1b). The proposed facilities are the Strategic Computing Center (SCC) and the Nonproliferation and International Security Center (NISC). This work is part of a broader program of geologic studies that seek to quantify probabilistic seismic hazards, including ground motion and surface rupture, at the Laboratory.

The objective of this drilling program was to intercept stratigraphic contacts within the Tshirege Member of the Bandelier Tuff and to evaluate if measurable stratigraphic separation ("offset") of those contacts was caused by faulting between drill sites. Geologic cores removed from the holes were used to define and correlate the stratigraphic sequence at each drillhole to aid in identifying geologic structure that might impact the buildings' foundations and stability in the future. Near-surface faults that have the potential for surface-rupture in the event of large earthquakes could affect the integrity of building foundations and structures.

Figure 1b. Upper map shows the outline of Los Alamos National Laboratory with Technical Areas outlined in black. Technical Area-3 (TA-3) is shaded grey. Lower map shows the location of the boreholes (black dots) for the proposed SCC and NISC buildings in TA-3.

The borehole locations and the proposed (April 1998) outlines (footprints) of the SCC and NISC buildings (Chavez-Grieves, 1998) in TA-3 are shown in Figure 1c. Borehole names and coordinates (New Mexico State Plane reference) are listed in Table 1. Borehole locations were selected based on size and shape of the building footprints, with allowances made for the presence of buried electrical utilities, water pipelines, radioactive waste pipelines, and communication lines. Utilities were located using as-built drawings and visual inspections and by use of induced radio-frequency detection (Metratech 810 detector), typically used for locating shallowly buried utility lines.

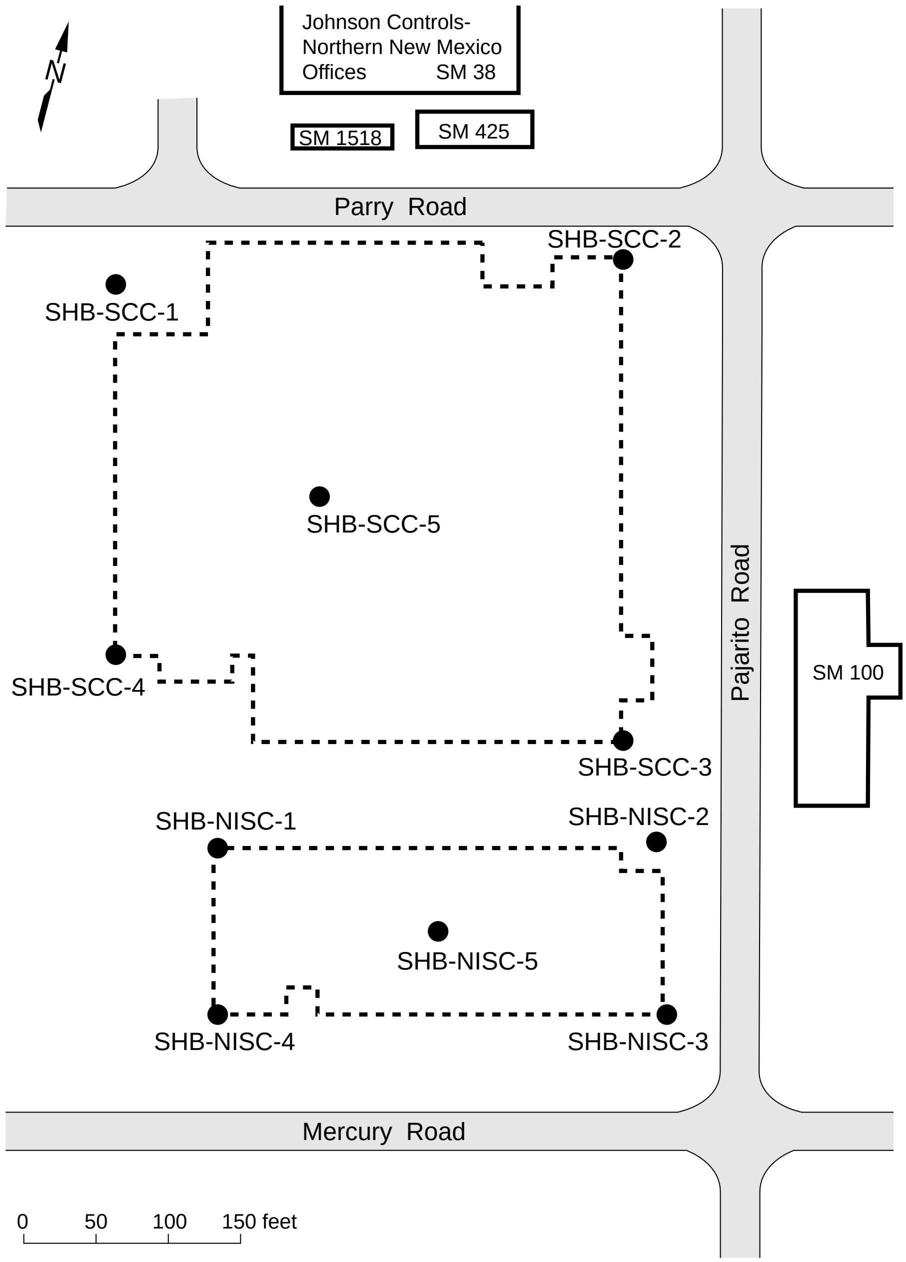

Figure 1c. Borehole locations, proposed building outlines (dashed lines), and nearby buildings (solid lines) with number designations.

II. METHODS

Drilling and coring operations took place from March 30 to April 13, 1998. The holes were augered in 2.5-ft core lengths using a hollow-stem auger with a split-spoon barrel and wireline retrieval system powered by a CME Model 750 rig. Core diameter was 3.5 in. A total of 847.5 ft was drilled in 11 days with 96% core recovery. Daily operations at the rig were supported by a crew of three drillers, two geologists, and a site safety professional. The excellent core recovery can be attributed to driller familiarity with the type of rock present, careful drilling with emphasis on core recovery, and the shallow target depth (<100 ft) for each hole. In spite of the excellent recovery, core cohesiveness was poor in intervals where the tuff was poorly welded. The combined effects of drilling, sample rheology, and handling rendered most samples to loose powder when transferred to archive boxes. Consequently,

Table 1. Coordinates for the ten SCC and NISC boreholes.

Borehole	Northing (ft)	Easting (ft)	Ground Elev. (ft)
SHB-SCC-1	1773532.61	1617472.83	7440.24
SHB-SCC-2	1773621.48	1617818.29	7430.54
SHB-SCC-3	1773297.36	1617876.36	7428.13
SHB-SCC-4	1773296.73	1617515.47	7441.85
SHB-SCC-5	1773433.34	1617634.30	7435.71
SHB-NISC-1	1773179.06	1617595.94	7439.24
SHB-NISC-2	1773233.30	1617903.11	7428.15
SHB-NISC-3	1773115.09	1617929.48	7427.82
SHB-NISC-4	1773058.30	1617617.11	7439.29
SHB-NISC-5	1773148.02	1617769.11	7432.46

many primary sample textures that were observable in the drill spoon did not survive the transfer to the core box. Detailed lithologic logs were prepared for each hole at the drill sites upon retrieval of the core and supplemented with later detailed examination of key intervals at LANL's Environmental Restoration Project Field Support Facility where the cores are archived. Cores were marked and boxed at the drill sites using a procedure designed by Goff (1986) as guidance. The logs include descriptions of lithology, fractures, fracture fill, texture, and mineralogy, and the locations of samples taken for chemical analyses.

Major and trace elements were analyzed for 57 bulk-rock samples using an automated Rigaku wavelength-dispersive x-ray fluorescence (XRF) spectrometer. Samples were first crushed and homogenized in 15- to 20-g portions in a tungsten-carbide shatterbox in accordance with Yucca Mountain Project procedure LANL-EES-DP-130 — Geologic Sample Preparation. Sample splits were heated at 110°C for 4 hrs, and then allowed to equilibrate with ambient atmosphere for 12 hrs. One gram splits were fused at 1100°C with 9 g of lithium tetraborate flux to obtain the fusion disks. Additional one gram splits were heated at 1000°C to obtain the loss-on-ignition (LOI) measurements. Elemental concentrations were calculated by comparing x-ray intensities for the samples to those for 21 standards of known composition. A fundamental parameters program was used for matrix corrections (Criss, 1980). The XRF method that was employed calculates the concentrations of ten compounds (SiO_2, TiO_2, Al_2O_3, Fe_2O_3, MnO, MgO, CaO, Na_2O, K_2O, P_2O_5), ten minor elements (V, Cr, Ni, Zn, Rb, Sr, Y, Zr, Nb, Ba), and loss-on-ignition (LOI). As discussed below, the compositional data were used to confirm and (or) tighten control on elevations of the geologic contact between Unit 4 and Unit 3 of the Tshirege Member of the Bandelier Tuff.

III. STRATIGRAPHY AND NOMENCLATURE

The stratigraphic units of the Bandelier Tuff described in this report are largely according to Broxton and Reneau (1995). We have encountered units of more local importance such as transitional units identified by Warren et al. (1998). The Bandelier Tuff (Figure 2) is dominantly composed of a complex sequence of nonwelded to welded ignimbrites that were erupted from the Valles-Toledo caldera complex (Griggs, 1964; Smith and Bailey, 1966; Smith et al., 1970; Gardner et al., 1986). Beneath the Laboratory, the Bandelier Tuff consists of two members: the lower Otowi Member (1.61 Ma; Izett and Obradovich, 1994) and the upper Tshirege Member (1.22 Ma; Izett and Obradovich, 1994), separated by a unit of volcaniclastic rocks and tuffs of the Cerro Toledo interval (Smith et al., 1970; Heiken et al., 1986; Broxton and Reneau, 1995, Lavine et al., 1997). The Tshirege Member consists of at least four mappable units (Units 1 through 4). Clay-rich soils and sediments overlie Unit 4 and form the surface deposits at

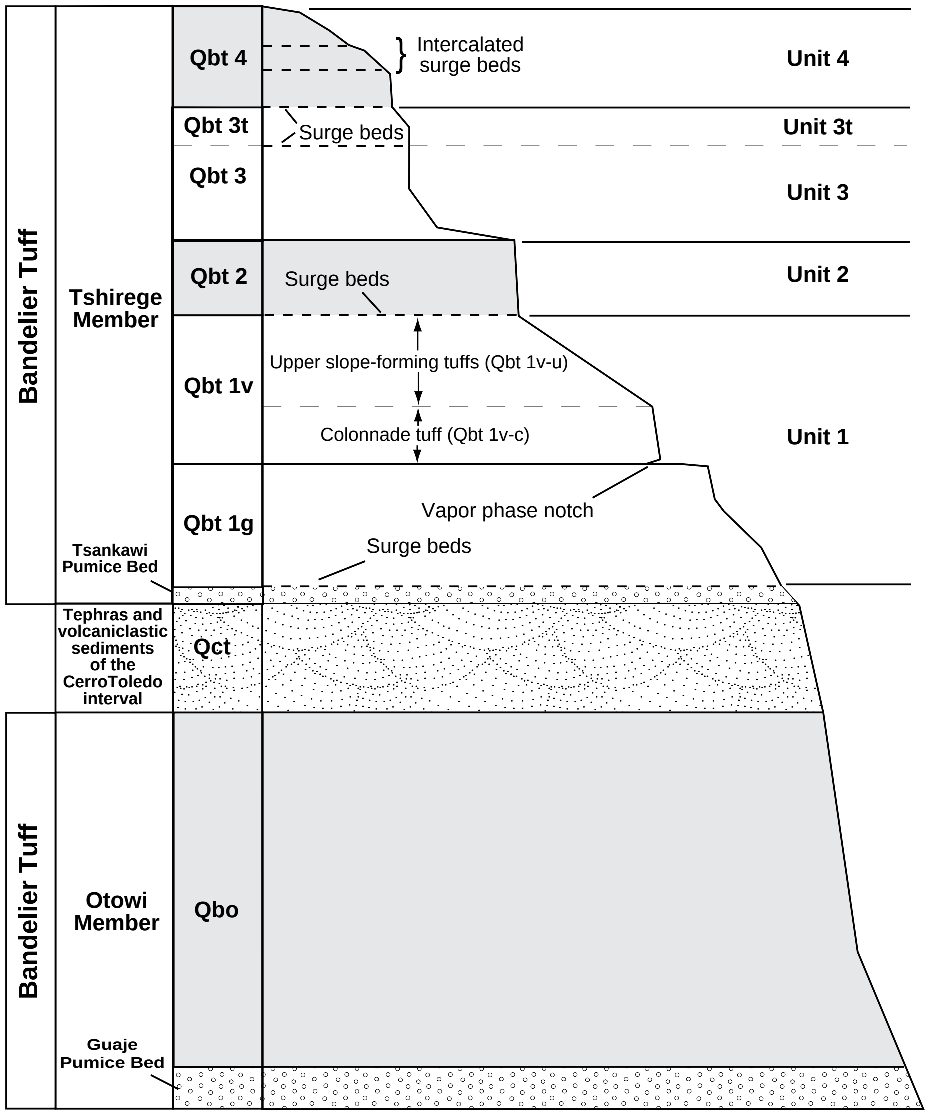

Figure 2. Composite stratigraphy of the Bandelier Tuff on the Pajarito Plateau, modified from Broxton and Reneau (1995). At any given locality, units can pinch out or swell in thickness. Note the surge beds at various unit boundaries and within Unit 4. The SCC and NISC boreholes penetrated Units 4, 3t, and 3 only.

the drill site. The ten boreholes were designed to penetrate Unit 4 and identify the contact between units 3 and 4. The thickness of Unit 4 in this locality ranges from about 70 to 80 ft. Table 2 lists the boreholes, their total depths, and the contact depths/elevations resulting from the drilling and analysis.

In the SCC and NISC boreholes, the contact between Unit 4 and Unit 3 can be transitional in both texture and mineralogy, and the designation *Unit 3t* is used to delineate this interval between the base of Unit 4 and Unit 3. Unit 3t has been recognized in outcrops in upper Los Alamos Canyon, located 0.5 mi north of the drill site, and has been shown to be geochemically transitional between units 4 and 3, particularly with regard to silica, titanium, zirconium, and barium contents (D.E. Broxton and J.N. Gardner, personal communication; Warren et al., 1997). At the drill site, Unit 3t varies from 0 ft to 4.2 ft thick and may represent a thin, local depositional lobe. Unit 3t thickness increases to about 40 ft in exposures in Los Alamos Canyon. In order to eliminate any effects of an irregular lobe of Unit 3t from the interpretation of the area, the top of Unit 3 is chosen to define the geologic surface used for the structural analysis in this report.

Table 2. Borehole designations, total depths, and significant stratigraphic contact depths.

Borehole	Total Depth (ft)	Units 4/3 Contact Depth (ft)	Units 4/3 Contact Elev. (ft)	Surge Interval (ft)	Units 4/3t Contact Depth (ft)	Units 4/3t Elev. (ft)	Units 3t/3 Contact Depth (ft)	Units 3t/3 Elev. (ft)	Unit 3t thickness (ft)
SHB-NISC-1	82.5	--	--	74.9-75.5	75.5	7363.7	76.8	7362.4	1.3
SHB-NISC-2	82.5	74.8	7353.3	72.5-74.8	--	--	--	--	0
SHB-NISC-3	75.0	--	--	69.7-69.8	69.8	7358.0	74.0	7353.52	4.2
SHB-NISC-4	82.5	--	--	70.8-71.0	71.0	7368.3	75.0	7364.29	4.0
SHB-NISC-5	85.0	--	--	73.3-73.4	73.4	7359.1	74.7	7357.76	1.3
SHB-SCC-1	97.5	80.0	7360.2	77.5-80.0	--	--	--	--	0
SHB-SCC-2	85.0	--	--	78.3-79.0	79.0	7351.5	79.8	7350.74	0.8
SHB-SCC-3	85.0	--	--	73.2-73.6	73.6	7354.5	76.0	7352.13	2.4
SHB-SCC-4	90.0	--	--	--	78.4	7363.4	80.5	7361.35	2.1
SHB-SCC-5	82.5			76.0-76.3	76.3	7359.4	77.5	7358.21	1.2

IV. LITHOLOGIC DESCRIPTIONS

Field descriptions were supplemented by binocular microscope examinations of cores at the LANL Field Support Facility. Except for differences in texture and induration brought about by the variations in welding (as qualitatively determined by degree of pumice flattening), the lithologic descriptions of Units 3, 3t, and 4 are consistent from hole to hole. Lithologic descriptions are arranged in order from oldest to youngest rocks. Color references follow descriptions in the Rock-Color Chart (Geological Society of America, 1980). Specific characteristics of welding degree, unit assignments, and surge locations for each borehole are depicted in Figure 3.

Unit 3 Lithologic Description

Unit 3 is a nonwelded to moderately welded, pumice-poor, phenocryst-rich, devitrified tuff. During this drilling operation, the entire thickness of the unit was not penetrated; rather, a short interval (6 to 18.5 feet) of Unit 3 was cored to confirm the Unit 4/Unit 3 boundary by visual observations and geochemical analyses.

Phenocrysts in Unit 3 are abundant at 25 to 35 vol%, with quartz and alkali feldspar in subequal amounts, with very minor plagioclase. Phenocrysts are both larger, averaging 4 mm across, and more abundant than in Unit 4. The quartz and feldspar phenocrysts have the same distinctive physical characteristics as described for Unit 4 (bipyramidal quartz, chatoyant feldspar). Mafic phenocrysts are extremely rare, with those observed appearing to be very fine-grained hornblende.

Pumices within the Unit 3 ash flow range from 4 to 7 vol%. Lithic fragments are rare and make up less than 1 percent of the tuff.

Unit 3 is nonwelded at the top but grades rapidly downward to moderately welded tuff over a short interval (approximately 12 feet). Pumices are fully inflated and vesicular at the top of this unit, but with increased welding, the tubular pumice structures become progressively more deformed and flattened. Pumices are devitrified, primarily dark gray or light brown, and range in size from 5 mm to over 7 cm.

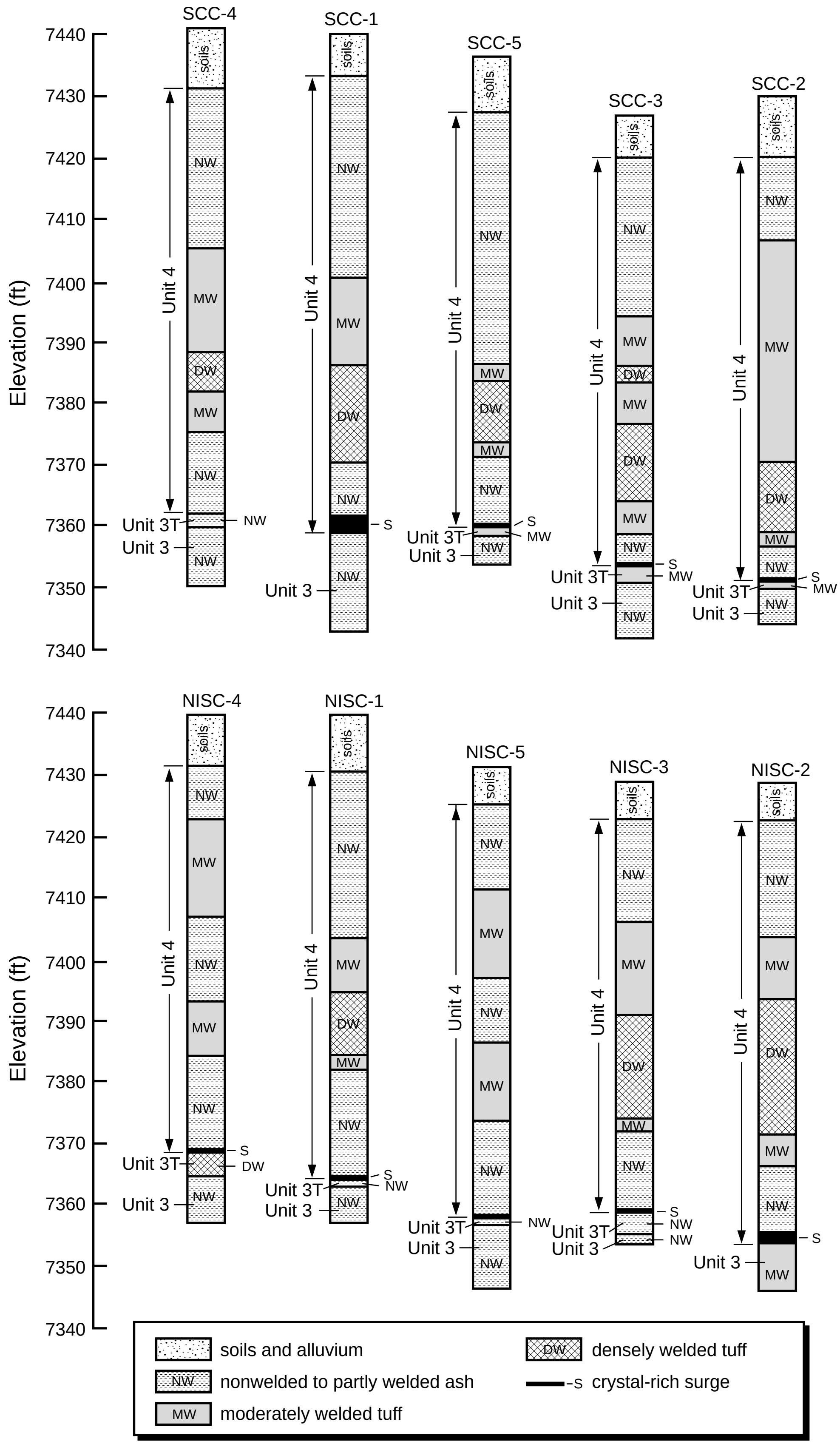

Figure 3. Stratigraphic columns and surge locations for SCC and NISC boreholes.

The matrix of Unit 3 is composed of ash, devitrified glass shards, crystal fragments, and very small pumice fragments. Matrix color ranges from pinkish gray to pale gray, and the matrix makes up approximately 65 vol% of the ash flow.

Unit 3t Lithologic Description

Unit 3t lies between Unit 3 and Unit 4. In hand sample, the most obvious difference from Unit 3 is its lower phenocryst percentage, which was used as the major criteria to identify Unit 3t. This unit has a phenocryst volume of 18% to 25%, which is transitional between Unit 3 and Unit 4. The other variant observed sporadically in Unit 3t is the presence of large, light gray flattened pumices. These pumices can extend across the core sample and give white banding to portions of the tuff. The pumices are flattened and devitrified. Unit 3t exhibits a moderately to densely welded character within the drilled area. Unit 3t varies from 0 to 4.2 ft thick in the boreholes and averages 1.7 ft thick. The recognition of the presence of Unit 3t increases the reliability that structural contours drawn on the top of Unit 3 are depicting a surface that was formed during a single depositional event. Calculating contours on the top of Unit 3 removes the effects of a depositional lobe of varying thickness of Unit 3t.

Unit 4 Lithologic Description

Unit 4 consists of nonwelded to densely welded, moderately pumice-rich, and phenocryst-poor to moderately phenocryst-rich, devitrified ignimbrite. Both phenocrysts and pumices range from 8 to 15 vol%. Lithic clasts are rare throughout the ash flow, typically representing less than 1 vol%. Color ranges from grayish pink (5R 8/2) to pale red (5R 6/2) to moderate pink (5R 7/4).

Welding varies within the unit, with a nonwelded to partly welded interval at the top, becoming moderately to densely welded (typically in the 40- to 70-foot-depth range) and then becoming nonwelded near the bottom of the unit. The upper nonwelded to partly welded interval can resemble a nonindurated pumiceous ash more than a consolidated tuff, particularly in the northwest drilling area, and several unconsolidated core intervals simply settled in the drill spoon under their own weight. A thin, crystal-rich, medium to coarse-grained unconsolidated sandy surge deposit is typically present at the base of Unit 4.

Phenocrysts in Unit 4 are dominantly quartz and sanidine, with minor plagioclase and altered mafic minerals. Unbroken quartz crystals are bipyramidal, approximately 2 mm on edge, and make up 5 to 7 vol% of the tuff. More than half the population of all crystal types is broken fragments. Sanidines are similar to quartz in size (2 to 3 mm) and abundance (approximately 5 vol%), and are chatoyant in sunlight. The rare and small (<1 mm) mafic phenocrysts comprise only 1 to 2 vol% of the tuff.

Pumices in Unit 4 range in size from 5 mm to greater than 6 cm and are deep brown or purple with gray cores. All the pumices are devitrified. Pumices in the upper portion of Unit 4 are vapor-phase altered and are characterized by minute acicular crystals growing within relict tubular structures of the pumice. The primary vapor-phase mineralogy is presumably cristobalite, tridymite, and sanidine. Pumices in the nonwelded to partly welded portions of this unit are fully inflated and show little or no deformation, but primary pumice textures are largely obliterated by devitrification and growth of vapor-phase minerals. In the central portion of the boreholes (approximately 40 to 70 feet) where welding is moderate to dense, the pumices are significantly elongated and aligned parallel to bedding. Their color is either dark gray or orange-pink, similar to the ash matrix. There is a rhythmic color banding in the lower portion of Unit 4 (typically at a depth of from 60 to 70 feet). The horizontal bands consist of a moderate brown color alteration of the tuff on a 1- to 2-cm scale alternating with the more typical orange-pink matrix.

In hand specimens, lithic fragments in Unit 4 are rare, typically less than 1 vol% of the tuff, and less than 8 mm in diameter. Some fragments are identifiable as dacite. Some lithic fragments are altered to a powdery lime-green material surrounded by an intense white alteration rim extending several millimeters into the enclosing tuff matrix. Despite their low volume percentage, these lithic fragments are present throughout the Unit 4 cores.

The matrix of Unit 4 is composed of ash, devitrified glass shards, small pumice fragments, and minute phenocryst fragments. The prevalent colors of the matrix in Unit 4 are grayish pink to moderate pink to pale red. The induration of the cores does not always match the degree of welding. Much of the moderately to densely welded core was recovered as 2- to 5-cm thick discs of indurated rock surrounded by rock powder in the core barrel, an effect caused by drilling action. Some of the other drill hole locations (SHB-NISC-4 in particular) yielded moderately to densely welded core that was relatively friable.

The sandy surge deposit at the base of Unit 4 was identified in nine of the ten core holes drilled. The surge was not identified in hole SHB-SCC-4. It typically is 1 to 12 in. thick, but in SHB-SCC-1 is about 30 in. thick. The surge interval is typically composed of greater than 80 vol% quartz and feldspar crystals and ~20% ash. Recovery of undisturbed surge is difficult because of its noncohesive, granular nature, but most of these intervals appear as massive, well sorted, and poorly indurated sand. One intact core sample from SHB-SCC-3 exhibits laminar beds or low-angle cross-beds.

Post-Bandelier Sediments and Soils

Sediments overlying Bandelier Tuff at the drill site consist of moderate reddish brown (10R 4/6) dense, massive clays and subordinate clay-rich soils with variable (5 to 25 vol%) amounts of silt and sand-sized grains. The thickness of the sediments ranges from 5.5 to 8.9 ft, and well-developed soil horizons within the package of sediments make up less than 10% of the volume encountered in the cores. The massive dark-brown clay beds contain rare, white, nonwelded pumice fragments, usually less than 1/4-inch diameter, but all other ash components of the sediments have been completely altered to clays. Some intervals up to 3 ft thick contain nearly 100% clay material. Soil horizons are from 1 to 5 in. thick, but are not common in the cores and do not appear continuous from hole to hole. Toward the base of the sediments, angular, oxidized, and gravel-sized pieces of deeply weathered tuff become more common in the clay-rich core as the interface with Bandelier Tuff is approached. The contact with underlying Bandelier Tuff is usually transitional, marked by an interval of deeply weathered tuff extending from 3 ft to as much as 6 ft thick. Typically, the sediments above the tuff are moist, although no water-producing zones were found at any elevation during drilling. The sediments are capped with 2 to 5 in. of asphalt for the parking lot that occupies the site.

V. GEOCHEMISTRY

Bulk-rock chemical compositions for tuffs near contact zones in the ten SHB-SCC and SHB-NISC boreholes are given in Table 3. Previous whole-rock analyses from borehole 49-2-700-1 at TA-49 demonstrate that Unit 4 can be distinguished from Unit 3 in both major and trace element chemistry

(Warren et al., 1998; Stimac et al., in preparation). An increase in SiO_2, and decreases in TiO_2, Zr, Ba, and Sr, mark the transition from Unit 4 to underlying Unit 3 (Figure 4). Guided by hand-specimen mineralogy, the presence of the surge layer at the base of Unit 4, and the recognition of transitional Unit 3t, we concentrated our sample points across the suspected contacts. The variations in SiO_2, TiO_2, Zr, and Ba across the units, together with the presence of the surge at the base of Unit 4, help determine the elevations of the Unit 4/Unit 3t and Unit 3t/Unit 3 contact surfaces with high degrees of accuracy.

In addition to variation in elemental concentrations, borehole 49-2-700-1 samples show a compositional gap between Unit 4 and Unit 3 with respect to TiO_2 between about 0.24 wt% and 0.14 wt%. Other elements also show distinct compositional variation across this contact. However, at TA-3 the compositional gap is bridged somewhat by the presence of Unit 3t, a thin tuffaceous interval with transitional chemistry and petrography. Where present, Unit 3t is located above Unit 3 and beneath the Unit 4 surge. Texturally, Unit 3t is distinguished from Unit 4 by increased phenocryst size and content, but lesser phenocryst content than the underlying Unit 3, which has a crystal-rich appearance with 25 to 35 vol% crystals. Chemically, Unit 3t has between about 0.15 to 0.18 wt% TiO_2 and also shows transitional contents of Ba, Rb, Zr, and SiO_2. Unit 3t and other subunits within the Tshirege Member have been chemically documented in Warren et al. (1998).

Unit 3t was not recognized in borehole 49-2-700-1 by either textural or chemical analysis. The absence of this unit may be attributed to nondeposition at that locality, or possibly because of the 10-ft sampling interval employed for that borehole.

SiO_2, TiO_2, Zr, and Ba concentration variations across the contact are discussed in the following paragraphs in support of the elevations determined for the surface of interest.

Silica

SiO_2 contents in the SHB-SCC and SHB-NISC cores across the Unit 4/Unit 3 contact are shown in Figure 5. In borehole 49-2-700-1, SiO_2 contents average about 74% in Unit 4 and 77% in Unit 3. At the SCC-NISC building site, SiO_2 also averages about 74% in Unit 4 and 77% in Units 3 and 3t. Unit 3 is a high-silica rhyolite whose increased silica is reflected in an increase in abundance of quartz crystals in the phenocryst population. An apparent SiO_2 gap is recorded in the SHB-SCC core data, whereas the SHB-NISC data suggest a more complete record of increasing SiO_2 down-section.

Titanium

TiO_2 concentrations range from 0.28 to 0.11 wt% in samples from the ten cores, and show decreasing concentration on the order of 50% across the Unit 4/Unit 3 boundary (Figure 6). Unit 3t is represented by compositions between 0.15 and 0.18 wt% TiO_2. Few samples of Unit 3t are represented in these plots because of the limited thickness and the sampling interval. The Unit 4/Unit 3 contact is documented in each borehole by the drop in titanium concentrations across the location of the surge intervals (see Table 2 and Figure 2).

Unit 4 TiO_2 contents in the cores range from 0.28 down to 0.20 wt% TiO_2, whereas TiO_2 in Unit 4 in borehole 49-2-700-1 does not fall below 0.24 wt% TiO_2. This might be due to nondeposition of early Unit 4 ignimbrites lower in the eruption sequence at TA-49, or again it may be an artifact of the 10-ft sampling interval in hole 49-2-700-1.

Table 3. X-ray fluorescence analyses for 57 samples from SCC and NISC boreholes.*

Sample Number	Depth (ft)	Sample Elev. (ft)	Unit	SiO_2 wt%	TiO_2 wt%	Al_2O_3 wt%	Fe_2O_3 wt%	MnO wt%	MgO wt%	CaO wt%	Na_2O wt%	K_2O wt%	P_2O_5 wt%	LOI % wt%
SHB-SCC-1/69.0	69.0	7371.2	4	74.61	0.24	12.96	2.11	0.07	0.17	0.60	4.52	4.65	0.04	0.16
SHB-SCC-1/75.0	75.0	7365.2	4	74.66	0.25	13.26	2.20	0.07	0.18	0.66	4.46	4.58	0.04	0.23
SHB-SCC-1/77.5	77.5	7362.7	4	75.09	0.23	13.14	2.15	0.07	0.15	0.54	4.46	4.63	0.04	0.28
SHB-SCC-1/80.0	80.0	7360.2	3	77.10	0.15	12.36	1.78	0.06	0.11	0.42	4.24	4.41	0.02	0.21
SHB-SCC-1/81.5	81.5	7358.7	3	77.52	0.12	11.85	1.51	0.05	-0.11	0.36	4.23	4.39	-0.01	0.04
SHB-SCC-1/84.8	84.8	7355.4	3	77.46	0.13	12.04	1.52	0.06	-0.11	0.33	4.24	4.38	0.01	0.07
SHB-SCC-1/85.3	85.3	7354.9	3	77.12	0.13	12.20	1.59	0.06	-0.11	0.34	4.36	4.53	0.01	0.10
SHB-SCC-1/91.0	91.0	7349.2	3	76.41	0.14	12.43	1.69	0.07	-0.11	0.37	4.32	4.49	0.01	0.08
SHB-SCC-2/77.0	77.0	7353.5	4	73.88	0.28	13.51	2.52	0.08	0.28	0.65	4.09	4.46	0.05	0.73
SHB-SCC-2/78.0	78.0	7352.5	4	74.74	0.25	13.00	2.34	0.09	0.21	0.56	4.29	4.52	0.04	0.29
SHB-SCC-2/79.1	79.0	7351.5	3t	76.92	0.16	12.64	1.68	0.05	-0.11	0.35	4.18	4.46	0.02	0.28
SHB-SCC-2/81.5	81.5	7349.0	3	78.11	0.12	12.05	1.47	0.05	-0.11	0.30	4.04	4.32	0.01	0.18
SHB-SCC-2/84.0	84.0	7346.5	3	78.19	0.12	11.84	1.51	0.05	-0.11	0.29	3.97	4.29	0.01	0.14
SHB-SCC-3/70.8	70.8	7357.3	4	74.36	0.23	12.86	2.08	0.09	0.15	0.49	4.37	4.62	0.04	0.18
SHB-SCC-3/72.3	72.3	7355.8	4	75.19	0.23	13.00	2.22	0.08	0.17	0.59	4.35	4.42	0.03	0.16
SHB-SCC-3/74.2	74.2	7353.9	3t	77.21	0.14	12.09	1.63	0.06	-0.11	0.42	4.09	4.24	0.01	0.20
SHB-SCC-3/76.0	76.0	7352.1	3	77.26	0.13	12.46	1.58	0.05	-0.11	0.38	4.23	4.49	0.01	0.10
SHB-SCC-3/80.7	80.7	7347.4	3	77.02	0.13	11.94	1.61	0.06	-0.11	0.36	4.12	4.38	0.01	0.14
SHB-SCC-4/74.0	74.0	7367.9	4	74.27	0.25	13.36	2.20	0.07	0.19	0.63	4.34	4.65	0.04	0.28
SHB-SCC-4/75.5	75.5	7366.4	4	74.27	0.25	13.37	2.35	0.07	0.22	0.56	4.17	4.54	0.04	0.62
SHB-SCC-4/77.4	77.4	7364.5	4	75.27	0.21	12.99	2.06	0.07	0.15	0.50	4.44	4.68	0.03	0.15
SHB-SCC-4/78.5	78.5	7363.4	3t	75.67	0.18	12.51	1.90	0.07	0.14	0.50	4.28	4.44	0.02	0.12
SHB-SCC-4/81.5	81.5	7360.4	3	77.46	0.14	12.39	1.65	0.06	-0.11	0.41	4.35	4.59	0.01	0.13
SHB-SCC-5/74.7	74.7	7361.0	4	75.09	0.21	12.86	1.94	0.06	0.12	0.50	4.31	4.66	0.03	0.16
SHB-SCC-5/75.2	75.2	7360.5	4	74.48	0.22	12.99	1.96	0.07	0.14	0.52	4.46	4.66	0.04	0.12
SHB-SCC-5/75.8	75.8	7359.9	4	74.63	0.22	12.85	2.10	0.07	0.15	0.53	4.40	4.63	0.04	0.14
SHB-SCC-5/76.5	76.5	7359.2	3t	75.21	0.19	12.79	2.10	0.07	0.19	0.59	4.28	4.34	0.03	0.27
SHB-SCC-5/78.2	78.2	7357.5	3	77.88	0.12	11.81	1.48	0.05	-0.11	0.37	4.16	4.33	0.01	0.10

* Concentrations preceded by a negative sign are below detection limits. Measurement uncertainties are available on request from the authors.

Table 3. (continued)

Sample Number	V ppm	Cr ppm	Ni ppm	Zn ppm	Rb ppm	Sr ppm	Y ppm	Zr ppm	Nb ppm	Ba ppm	Total Trace wt%	Total Major wt%	Total + LOI wt%
SHB-SCC-1/69.0	-9.94	-7.90	-10.06	71.23	81.25	66.86	33.41	336.74	52.29	340.61	0.12	99.97	100.25
SHB-SCC-1/75	11.94	-7.92	-10.05	81.12	90.87	70.45	36.77	345.96	50.79	306.15	0.12	100.36	100.71
SHB-SCC-1/77.5	-9.92	-7.93	-10.05	76.27	97.84	58.86	37.69	338.99	51.32	262.59	0.11	100.51	100.90
SHB-SCC-1/80	-9.74	-7.92	-10.06	65.50	89.79	44.47	31.90	269.42	50.45	273.95	0.10	100.65	100.96
SHB-SCC-1/81.5	-9.68	-7.90	-10.06	50.27	90.13	28.40	32.51	228.88	47.11	187.84	0.08	100.03	100.15
SHB-SCC-1/84.8	-9.68	-7.89	-10.07	45.28	100.33	33.46	33.44	232.66	57.16	144.01	0.08	100.17	100.32
SHB-SCC-1/85.3	-9.68	-7.87	-10.07	60.03	109.07	32.19	35.72	234.29	45.76	148.71	0.08	100.34	100.52
SHB-SCC-1/91.0	-9.69	-7.92	-10.70	55.63	109.37	38.28	27.62	255.20	53.24	138.99	0.08	99.93	100.09
SHB-SCC-2/77.0	13.16	-7.95	-10.71	87.09	98.13	78.65	42.68	333.94	46.44	343.12	0.13	99.80	100.65
SHB-SCC-2/78.0	-9.93	-7.94	-10.70	76.26	116.98	73.94	21.91	321.47	38.14	348.92	0.12	100.05	100.46
SHB-SCC-2/79.1	-9.68	-7.91	-10.06	45.59	89.27	35.75	37.06	265.91	50.98	172.38	0.09	100.45	100.82
SHB-SCC-2/81.5	-9.64	-7.92	-10.06	45.15	90.18	36.21	25.70	221.54	42.30	148.95	0.08	100.46	100.72
SHB-SCC-2/84	-9.63	-7.92	-10.06	40.68	109.49	32.43	36.25	233.76	47.49	134.16	0.08	100.29	100.51
SHB-SCC-3/70.8	-9.85	-7.93	-10.06	60.23	95.48	48.20	30.66	342.73	51.73	287.08	0.11	99.27	99.56
SHB-SCC-3/72.3	-9.83	-7.87	-10.69	64.33	75.41	57.24	31.53	322.25	42.17	253.16	0.10	100.28	100.55
SHB-SCC-3/74.2	-9.66	-7.89	-10.06	48.59	79.40	36.96	27.74	224.08	39.43	216.14	0.08	99.88	100.16
SHB-SCC-3/76.0	-9.63	-7.93	-10.06	40.13	101.58	32.86	49.48	242.06	57.08	143.97	0.08	100.59	100.77
SHB-SCC-3/80.7	-9.65	-7.97	-10.70	46.45	107.39	38.08	31.69	239.82	36.66	167.97	0.08	99.64	99.86
SHB-SCC-4/74	11.80	-7.91	-10.05	78.83	86.81	73.11	32.20	338.40	37.17	282.06	0.12	100.01	100.41
SHB-SCC-4/75.5	-9.92	-7.93	-10.69	80.56	98.51	63.03	36.23	343.65	45.45	329.52	0.12	99.84	100.58
SHB-SCC-4/77.4	-9.84	-7.95	-10.05	85.59	91.12	48.38	28.54	322.66	51.32	244.24	0.11	100.38	100.64
SHB-SCC-4/78.5	-9.80	-7.92	-10.05	70.61	80.10	49.83	28.55	291.25	35.06	215.69	0.10	99.71	99.92
SHB-SCC-4/81.5	-9.70	-7.92	-10.69	60.74	96.07	34.88	39.56	254.48	49.52	173.00	0.09	101.06	101.28
SHB-SCC-5/74.7	-9.77	-7.92	-10.05	62.89	93.12	43.65	25.00	341.40	44.96	248.96	0.11	99.79	100.05
SHB-SCC-5/75.2	-9.83	-7.95	-10.06	62.75	93.98	58.61	21.71	332.22	34.23	306.94	0.11	99.54	99.77
SHB-SCC-5/75.8	-9.89	-7.90	-10.05	72.69	94.88	55.65	37.59	337.99	41.06	243.73	0.11	99.62	99.87
SHB-SCC-5/76.5	14.98	-7.92	-10.05	75.72	82.99	55.83	27.96	269.04	44.36	306.92	0.11	99.78	100.16
SHB-SCC-5/78.2	-9.62	-7.87	-10.06	44.22	91.53	35.56	27.38	214.69	44.36	158.82	0.08	100.22	100.39

* Concentrations preceded by a negative sign are below detection limits. Measurement uncertainties are available on request from the authors.

Table 3. (continued)

Sample Number	Depth (ft)	Sample Elev. (ft)	Unit	SiO_2 wt%	TiO_2 wt%	Al_2O_3 wt%	Fe_2O_3 wt%	MnO wt%	MgO wt%	CaO wt%	Na_2O wt%	K_2O wt%	P_2O_5 wt%	LOI % wt%
SHB-NISC-1/70.0	70.0	7369.2	4	74.71	0.25	12.97	2.21	0.08	0.20	0.64	4.33	4.47	0.04	0.45
SHB-NISC-1/73.8	73.8	7365.4	4	75.12	0.20	12.72	1.91	0.07	-0.11	0.40	4.29	4.70	0.03	0.14
SHB-NISC-1/75.6	75.6	7363.6	3t	77.30	0.16	12.36	1.78	0.06	-0.11	0.45	4.29	4.39	0.02	0.08
SHB-NISC-1/77.1	77.1	7362.1	3	77.82	0.13	12.28	1.56	0.05	-0.11	0.37	4.23	4.44	0.01	0.10
SHB-NISC-2/72.0	72.0	7356.1	4	75.01	0.23	13.05	2.09	0.07	0.15	0.48	4.40	4.67	0.03	0.19
SHB-NISC-2/72.5	72.5	7355.7	4(?)	76.23	0.15	12.41	1.54	0.06	-0.11	0.38	4.12	4.58	0.01	0.18
SHB-NISC-2/73.5	73.5	7354.6	4	75.68	0.26	12.31	2.68	0.09	0.22	0.71	4.26	4.32	0.03	0.12
SHB-NISC-2/74.0	74.0	7354.1	4	75.56	0.28	12.41	2.87	0.11	0.28	0.79	4.27	4.26	0.04	0.03
SHB-NISC-2/74.3	74.3	7353.8	4	76.29	0.26	12.13	2.74	0.10	0.28	0.82	4.16	4.16	0.04	0.12
SHB-NISC-2/75.0	75.0	7353.1	3	78.17	0.12	11.91	1.44	0.05	-0.11	0.36	4.00	4.42	0.01	0.05
SHB-NISC-2/76.8	76.8	7351.4	3	76.92	0.12	12.07	1.57	0.06	-0.11	0.40	4.07	4.38	0.01	0.10
SHB-NISC-2/80.2	80.2	7347.9	3	78.28	0.12	11.79	1.46	0.05	-0.11	0.33	4.04	4.27	0.01	0.10
SHB-NISC-3/67.0	67.0	7360.8	4	74.46	0.22	13.09	2.09	0.08	0.16	0.51	4.43	4.69	0.03	0.11
SHB-NISC-3/69.5	69.5	7358.3	4	73.54	0.21	13.51	2.08	0.10	0.17	0.60	4.73	4.71	0.03	0.11
SHB-NISC-3/70.0	70.0	7357.8	3t	76.02	0.15	12.61	1.55	0.05	-0.11	0.37	4.26	4.59	0.02	0.07
SHB-NISC-3/71.0	71.0	7356.8	3t	77.01	0.15	11.85	1.74	0.09	0.17	0.55	4.09	4.12	0.02	0.17
SHB-NISC-3/74.5	74.5	7353.3	3	77.34	0.11	12.16	1.43	0.05	-0.11	0.36	4.22	4.38	0.01	0.12
SHB-NISC-4/70.0	70.0	7369.3	4	75.78	0.23	13.13	2.10	0.07	-0.11	0.45	4.46	4.68	0.04	0.19
SHB-NISC-4/72.5	72.5	7366.8	3t	75.09	0.17	12.50	1.82	0.07	-0.11	0.25	4.44	4.86	0.02	0.21
SHB-NISC-4/74.6	74.6	7364.7	3t	76.02	0.17	12.86	1.85	0.12	-0.11	0.23	4.36	4.81	0.01	0.17
SHB-NISC-4/74.9	74.9	7364.4	3t	76.48	0.15	12.70	1.85	0.12	0.11	0.25	4.29	4.74	0.01	0.29
SHB-NISC-4/75.0	75.0	7364.3	3	76.91	0.15	12.45	1.78	0.10	0.11	0.30	4.27	4.55	0.01	0.19
SHB-NISC-4/75.3	75.3	7364.0	3	77.71	0.12	11.94	1.49	0.07	-0.11	0.28	4.09	4.46	-0.01	0.12
SHB-NISC-4/77.0	77.0	7362.3	3	77.48	0.12	12.16	1.49	0.05	-0.11	0.31	4.19	4.46	-0.01	0.09
SHB-NISC-5/71.1	71.1	7361.4	4	75.22	0.23	13.26	2.03	0.08	0.15	0.51	4.53	4.73	0.03	0.17
SHB-NISC-5/72.6	72.6	7359.9	4	76.16	0.20	12.65	2.00	0.07	0.13	0.48	4.29	4.48	0.03	0.18
SHB-NISC-5/74.0	74.0	7358.5	3t	77.52	0.12	12.15	1.55	0.06	-0.11	0.38	4.18	4.46	0.01	0.06
SHB-NISC-5/75.5	75.5	7357.0	3	77.75	0.12	12.00	1.50	0.05	-0.11	0.35	4.09	4.40	0.01	0.07
SHB-NISC-5/77.5	77.5	7355.0	3	78.05	0.12	12.01	1.51	0.06	-0.11	0.32	4.07	4.43	-0.01	0.10

* Concentrations preceded by a negative sign are below detection limits. Measurement uncertainties are available on request from the authors.

Table 3. (continued)

Sample Number	V ppm	Cr ppm	Ni ppm	Zn ppm	Rb ppm	Sr ppm	Y ppm	Zr ppm	Nb ppm	Ba ppm	Total Trace wt%	Total Major wt%	Total + LOI wt%
SHB-NISC-1/70	17.46	28.00	-10.07	77.26	96.31	76.35	31.28	339.01	48.17	315.37	0.13	99.90	100.48
SHB-NISC-1/73.8	-9.85	-7.95	-10.05	65.95	98.07	44.84	32.56	341.17	45.04	215.29	0.10	99.43	99.67
SHB-NISC-1/75.6	-9.75	-7.90	-10.06	29.86	82.78	36.92	40.36	282.49	57.37	177.29	0.09	100.80	100.97
SHB-NISC-1/77.1	-9.71	-7.88	-10.06	33.95	104.05	35.31	39.65	249.75	47.71	144.06	0.08	100.90	101.08
SHB-NISC-2/72.0	13.64	-7.91	-10.05	70.16	99.21	50.30	27.04	360.06	47.32	301.54	0.12	100.18	100.49
SHB-NISC-2/72.45	-9.69	9.02	-10.70	46.91	91.64	30.81	43.78	269.13	60.24	197.05	0.09	99.47	99.74
SHB-NISC-2/73.5	-9.98	-7.90	-10.06	89.39	68.96	63.18	21.55	318.83	34.16	237.87	0.10	100.56	100.78
SHB-NISC-2/74.0	-10.05	11.49	-10.05	61.52	60.15	51.23	22.83	306.39	28.31	348.67	0.11	100.86	101.00
SHB-NISC-2/74.3	-9.96	-7.95	-10.06	67.97	66.49	64.61	21.08	320.98	33.74	353.90	0.11	100.98	101.21
SHB-NISC-2/75.0	-9.64	-7.92	-10.71	48.58	107.30	33.22	29.83	239.29	51.93	144.22	0.08	100.48	100.62
SHB-NISC-2/76.8	-9.65	12.44	-10.06	26.08	91.44	33.11	43.50	253.96	45.20	197.48	0.09	99.59	99.78
SHB-NISC-2/80.2	-9.65	10.39	-10.08	35.80	104.05	33.54	31.47	233.55	56.17	163.39	0.08	100.35	100.54
SHB-NISC-3/67.0	-9.85	14.42	-10.68	65.89	92.44	52.03	30.76	345.56	49.81	263.22	0.11	99.76	99.99
SHB-NISC-3/69.5	-9.82	-7.89	-10.05	61.15	79.38	59.72	37.44	313.76	35.35	365.48	0.12	99.68	99.91
SHB-NISC-3/70.0	-9.68	-7.88	-10.06	48.01	87.45	33.72	38.80	270.83	41.23	153.50	0.08	99.62	99.77
SHB-NISC-3/71.0	-9.67	12.84	-10.06	30.40	57.24	54.03	22.09	212.84	34.63	303.29	0.09	99.79	100.05
SHB-NISC-3/74.5	-9.64	-7.93	-10.06	42.69	92.52	34.54	32.88	219.38	48.40	187.95	0.08	100.05	100.26
SHB-NISC-4/70	-9.91	-7.94	-10.06	61.18	91.73	57.14	40.56	336.57	47.74	282.23	0.11	100.94	101.24
SHB-NISC-4/72.5	-9.77	-7.95	-10.69	61.41	102.75	23.37	34.89	321.95	51.78	162.49	0.10	99.23	99.53
SHB-NISC-4/74.6	-9.74	-7.92	-10.06	46.92	118.12	27.35	39.15	340.18	54.59	215.49	0.10	100.44	100.71
SHB-NISC-4/74.9	-9.72	-7.94	-10.07	57.52	117.89	24.28	39.02	305.30	60.45	167.36	0.10	100.71	101.09
SHB-NISC-4/75.0	-9.69	36.54	13.10	45.55	113.72	31.73	31.05	267.18	57.79	182.10	0.10	100.62	100.91
SHB-NISC-4/75.25	-9.65	-7.94	-10.69	38.52	101.01	30.32	42.63	234.39	41.56	119.97	0.08	100.15	100.35
SHB-NISC-4/77.0	-9.65	-7.90	-10.70	35.32	94.56	33.63	31.08	227.88	48.49	139.42	0.08	100.26	100.43
SHB-NISC-5/71.1	-9.90	-7.88	-10.70	65.45	97.95	59.68	26.73	350.75	39.09	219.51	0.11	100.78	101.06
SHB-NISC-5/72.6	-9.85	32.51	-10.71	82.68	87.26	45.50	30.66	298.10	39.79	244.08	0.11	100.50	100.78
SHB-NISC-5/74	-9.66	-7.89	-10.07	62.15	105.92	33.72	36.44	236.38	58.22	163.54	0.09	100.43	100.58
SHB-NISC-5/75.5	-9.67	-7.90	-10.06	45.04	99.42	31.86	36.36	220.23	44.03	168.45	0.08	100.28	100.43
SHB-NISC-5/77.5	-9.66	-7.91	-10.07	45.19	97.20	27.71	41.46	246.79	45.76	158.64	0.08	100.58	100.76

* Concentrations preceded by a negative sign are below detection limits. Measurement uncertainties are available on request from the authors.

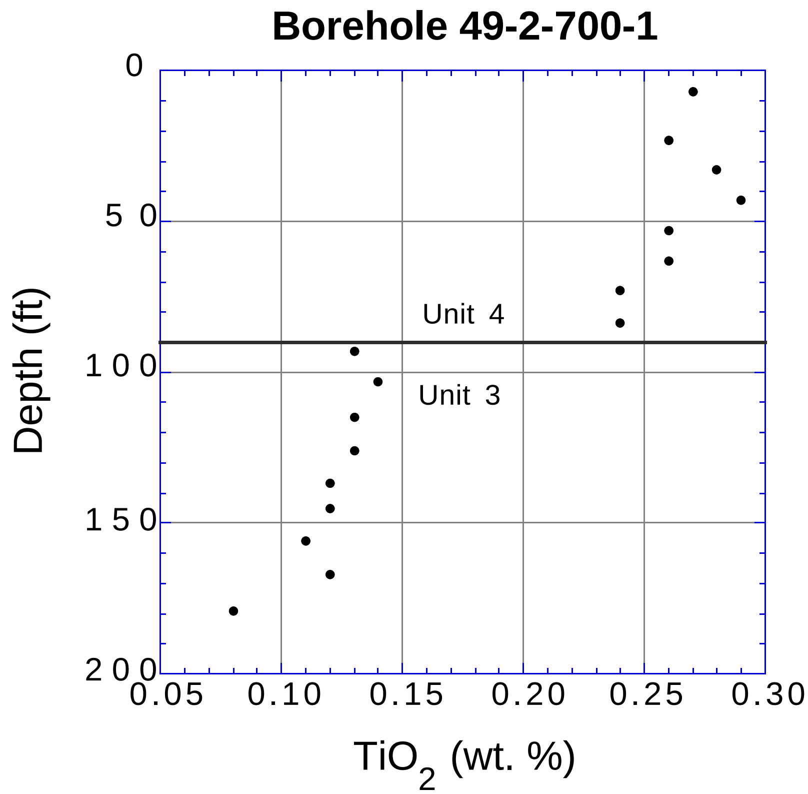

Figure 4. TiO_2 concentrations measured in Bandelier Tuff samples from borehole 49-2-700-1.

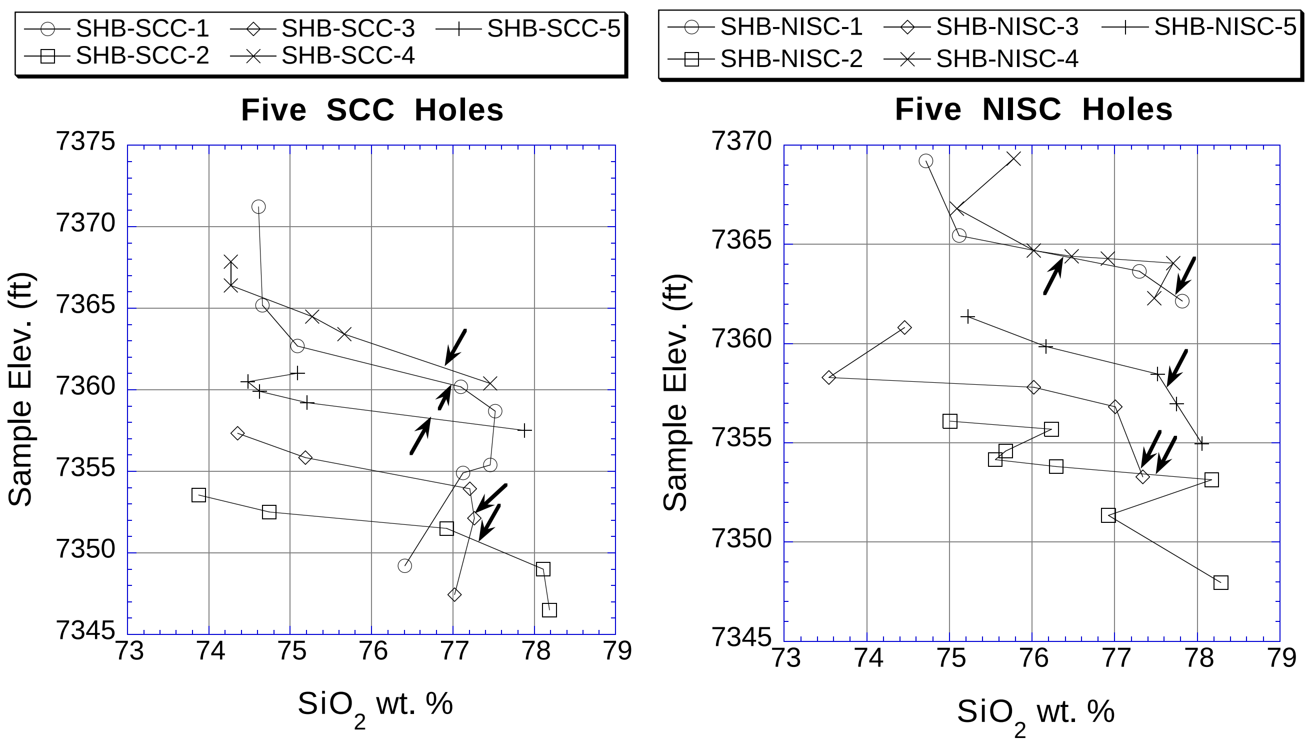

Figure 5. Percent SiO_2 versus sample elevations for SCC (left) and NISC (right) boreholes. Arrows denote the upper Unit 3 contact within each borehole.

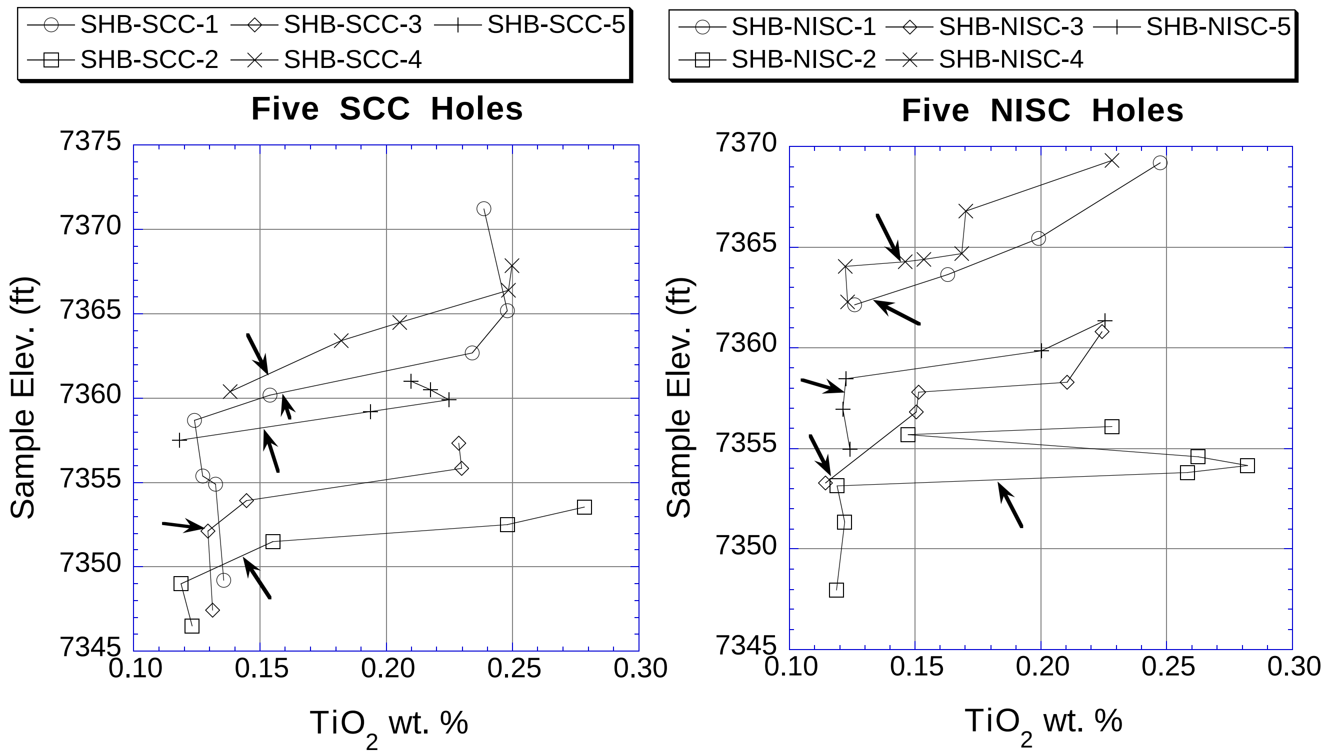

Figure 6. Percent TiO_2 versus sample elevations for SCC (left) and NISC (right) boreholes. Arrows denote the upper Unit 3 contact within each borehole.

Zirconium

Zr is another elemental guide to the Unit 4/Unit 3 contact (Figure 7). Zr shows a steep 30% decrease across the contact from Unit 4 to Unit 3 over the interval sampled. As with SiO_2 and TiO_2, the Zr concentrations of SHB-NISC series cores have a more complete transitional variation than in the SHB-SCC holes, suggesting a more complete depositional record of tuff beneath the southern (NISC) part of the drilled area.

Titanium and Barium

Ba concentration varies from a high of 365 ppm in SHB-NISC-2 (69 ft; Unit 4) to a low of 120 ppm in SHB-NISC-4 (75 ft; Unit 3). Barium versus TiO_2 plots show distinct groupings for Unit 4, Unit 3t, and Unit 3 in the northern half of the building site investigated, but the NISC analyses show a more complete chemical sequence of concentrations in these units (Figure 8). The groupings are further evidence of the consistent determination of the contact depths in each borehole.

VI. GEOLOGIC STRUCTURE

We have analyzed the three-dimensional positions of correlated stratigraphic markers among the bore holes to evaluate the possibility of vertical offsets caused by faulting beneath the facility sites. Computer-generated, three-dimensional surface models of the top of Unit 3 and inter-borehole cross sections are illustrative of these analyses.

A surface model of the top of Unit 3 was constructed using Surfer-32 software to determine the potential of faulting in the area of the SCC and NISC boreholes. The ten borehole locations and elevations of the

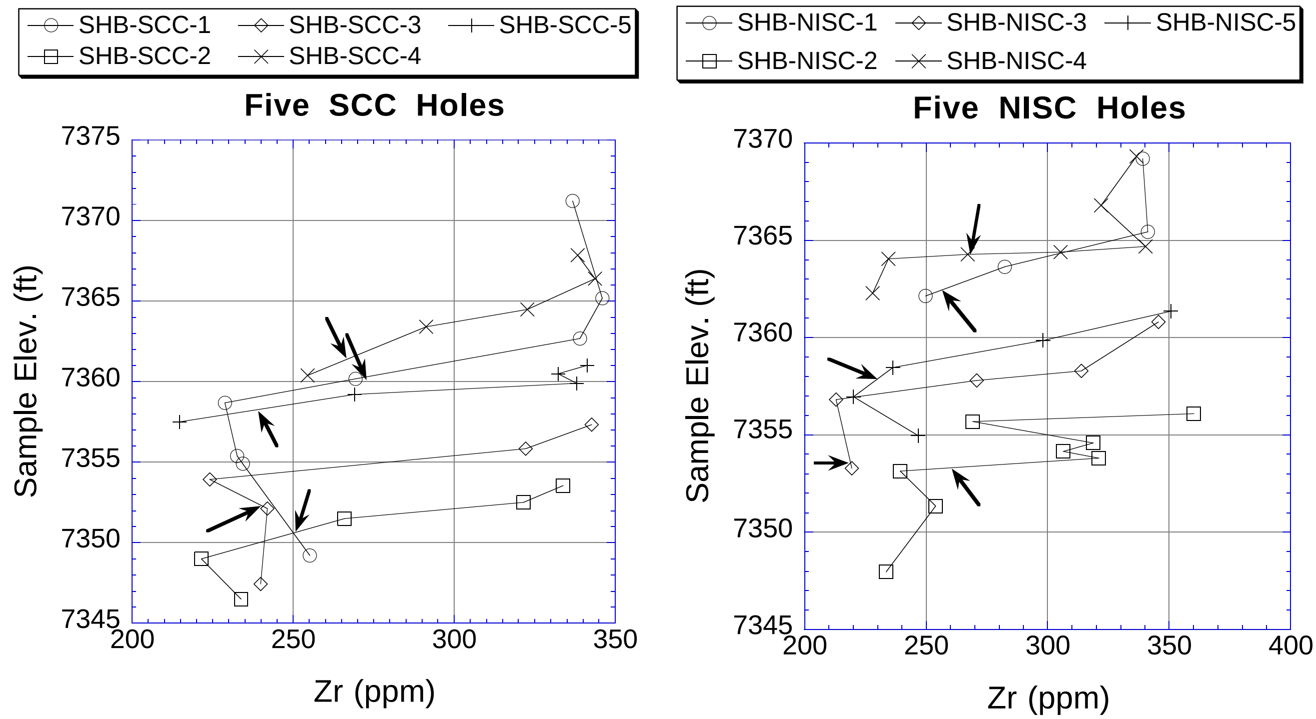

Figure 7. Zirconium concentration (ppm) versus sample elevation for SCC (left) and NISC (right) boreholes. Arrows denote the upper Unit 3 contact within each borehole.

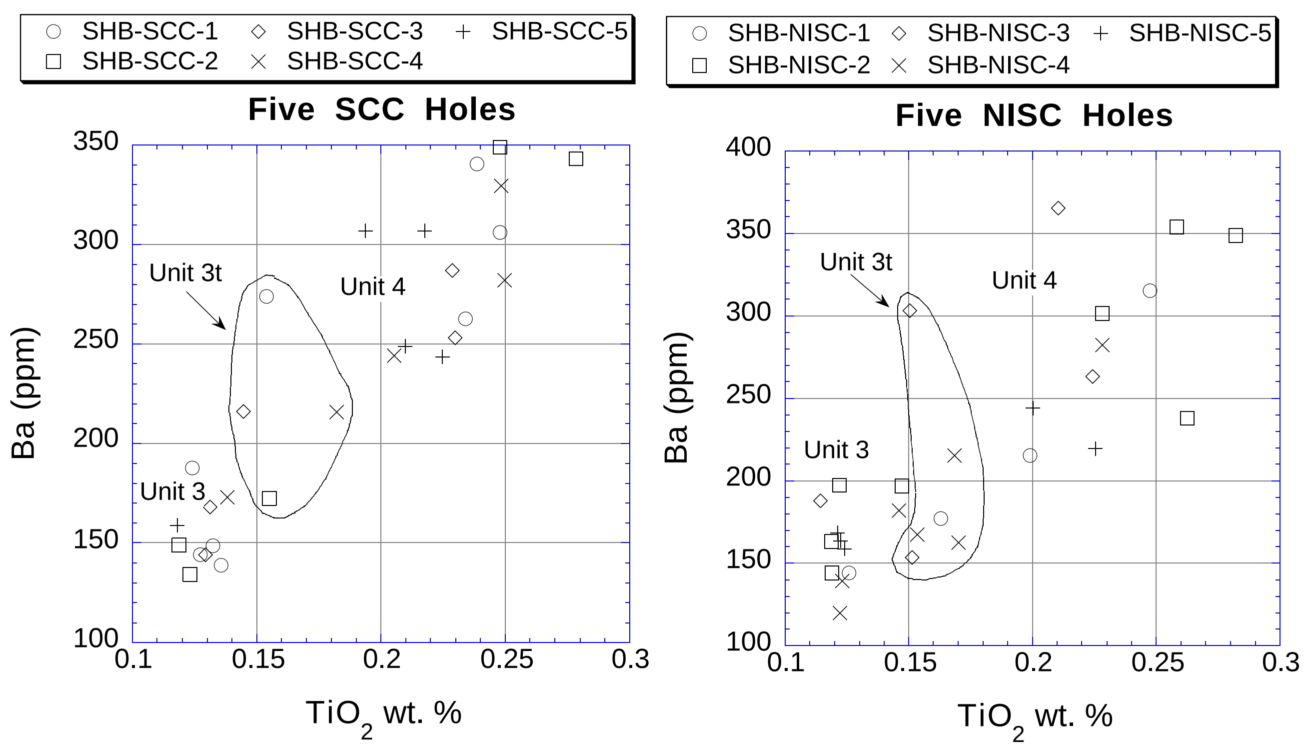

Figure 8. Percent TiO_2 versus barium concentration (ppm) for SCC (left) and NISC (right) boreholes showing distinct groupings of Unit 4, Unit 3t, and Unit 3 compositions.

surface of Unit 3 were used as input. The program uses kriging to interpolate the surface among control points, creating a model of the morphology and attitude of this contact. Figure 9 shows 1-ft-interval contours on the top of the modeled surface of Unit 3 for an area of approximately 9.6 acres. The surface of Unit 3 has an overall strike of about N68°E and a dip of 1.8°NE and shows no evidence of faults disrupting the morphology. The very shallow northeastward dip of the contact is consistent with the attitude of the contact in outcrops in neighboring Los Alamos and Two Mile canyons (north and southwest of the site, respectively).

The analysis suggests a small change in strike toward the northwest and an even shallower dip in the western third of the area. The rotation of strike to nearly east-west depicted in the southwest corner of Figure 9 is an artifact of the Surfer-32 interpolation among the fewer data points in the area. The Unit 3 surface shows minor irregularity in the southeast corner (SHB-SCC-3, SHB-NISC-2, and SHB-NISC-3). The approximately 1 foot difference in elevation of Unit 3 between boreholes NISC-2 and SCC-3

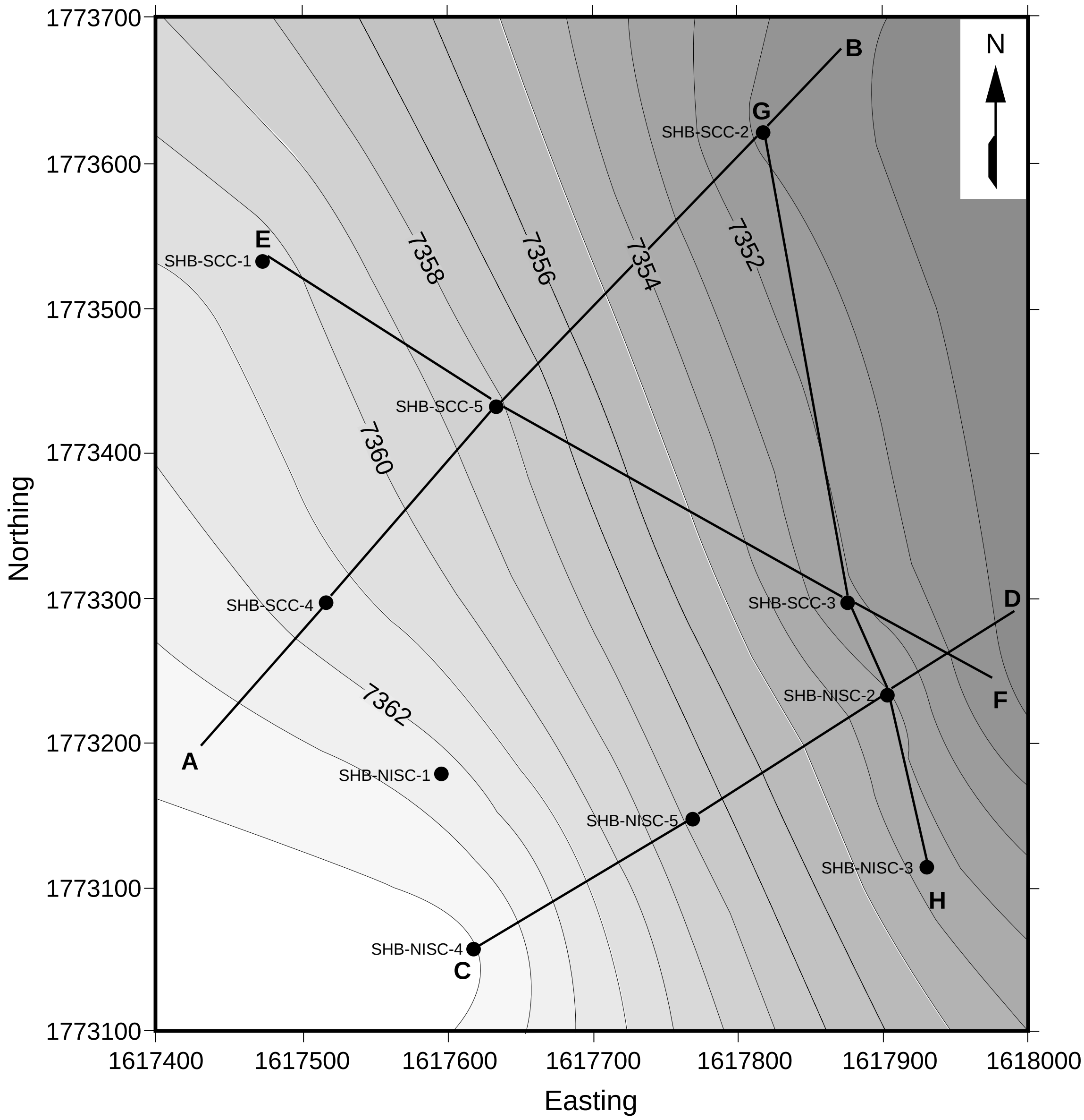

Figure 9. Contour map showing the top surface of Unit 3 in SCC and NISC boreholes, as modeled by Surfer 32 using kriging to interpolate the surface between control points (boreholes). Grid is in the State Plane Coordinate System, New Mexico Central Zone, 1983 North American Datum (in feet). Contour interval is 1 foot. The slope of the surface is to the east-northeast. Lines AGB, CD, EF, and GH are cross sections shown in Figure 10.

(1.4 ft difference over a distance of 70 ft) is within the known stratigraphic undulation of the contact surface and is not suspected of indicating a fault.

Figure 10 shows geologic cross sections drawn from the drill hole data, and depicts the contact surfaces dipping gently toward the northeast. Because the surfaces are dipping, all bends in each line of section show an abrupt change in apparent dip, but this is not related to faulting. There is no evidence of faulting through the block beneath the building sites.

VII. UNCERTAINTY ESTIMATE

Description of nearly complete cores from the ten closely spaced boreholes and use of published and unpublished information on the lithologic sequence within the upper Tshirege Member leave little uncertainty as to the accuracy of the pick of elevations for the unit contacts. The addition of 57 closely spaced samples for geochemical analysis and matching the chemistry with previously documented geochemical signatures of the unit boundaries yield further confidence that the contact elevations are accurate. We qualitatively estimate the uncertainty of the contact elevations in each borehole at ±1.0 ft.

The ten boreholes distributed over the relatively small area give good control for limiting the structural complexity beneath the building footprints. The small dip angle on the Unit 3 surface and the uniformity of the surface trend rule out the possibility of “large” faulting in the upper units of the Tshirege Member through the area between the boreholes. Although it is difficult to quantify the uncertainty, we feel confident that faults with greater than 2 ft of stratigraphic separation on the contact surface cannot be present beneath the building site.

VIII. CONCLUSIONS

Lithologic logging of nearly complete cores from ten boreholes and chemical analyses of 57 core samples have accurately defined a subsurface contact within the Bandelier Tuff over a 4-acre area covering the building sites for the proposed SCC and NISC buildings. The calculated orientation of this contact surface is consistent with surface exposures in the adjacent canyons and shows no evidence of disruption by faults with greater than about 2 ft of offset in the Bandelier Tuff. A fault or faults with less than about 2 ft of stratigraphic separation might not be detected by the current data sets.

These results provide a bound on a preliminary probabalistic seismic hazard analysis for potential surface fault displacement at TA-3 (Olig et al., 1998). There is no evidence from the cores that faulting is present at the SCC/NISC site. Nonetheless, if the southern end of the Rendija Canyon fault passes beneath the site, the cumulative displacement of Bandelier Tuff on the fault is between 0 and 2 ft and would correspond to the distributed or subsidiary faulting scenario.

IX. ACKNOWLEDGMENTS

Giday WoldeGabriel shared his experience in identifying differences among the various units in the Bandelier Tuff. Emily Kluk and Rick Warren (EES-1) performed the XRF analyses using the EES-1 group analytical facilities. The U.S. Department of Energy, through the Nuclear Weapons Technologies (NWT) Programs and the Nonproliferation and International Security (NIS) Division, provided funding for the coring and analysis of the results. Jim Holt (NWT) and Cliff Giles (NIS) were instrumental in securing funding for this project, and Larry Goen (ESA), and Doug Volkman (FSS) provided guidance

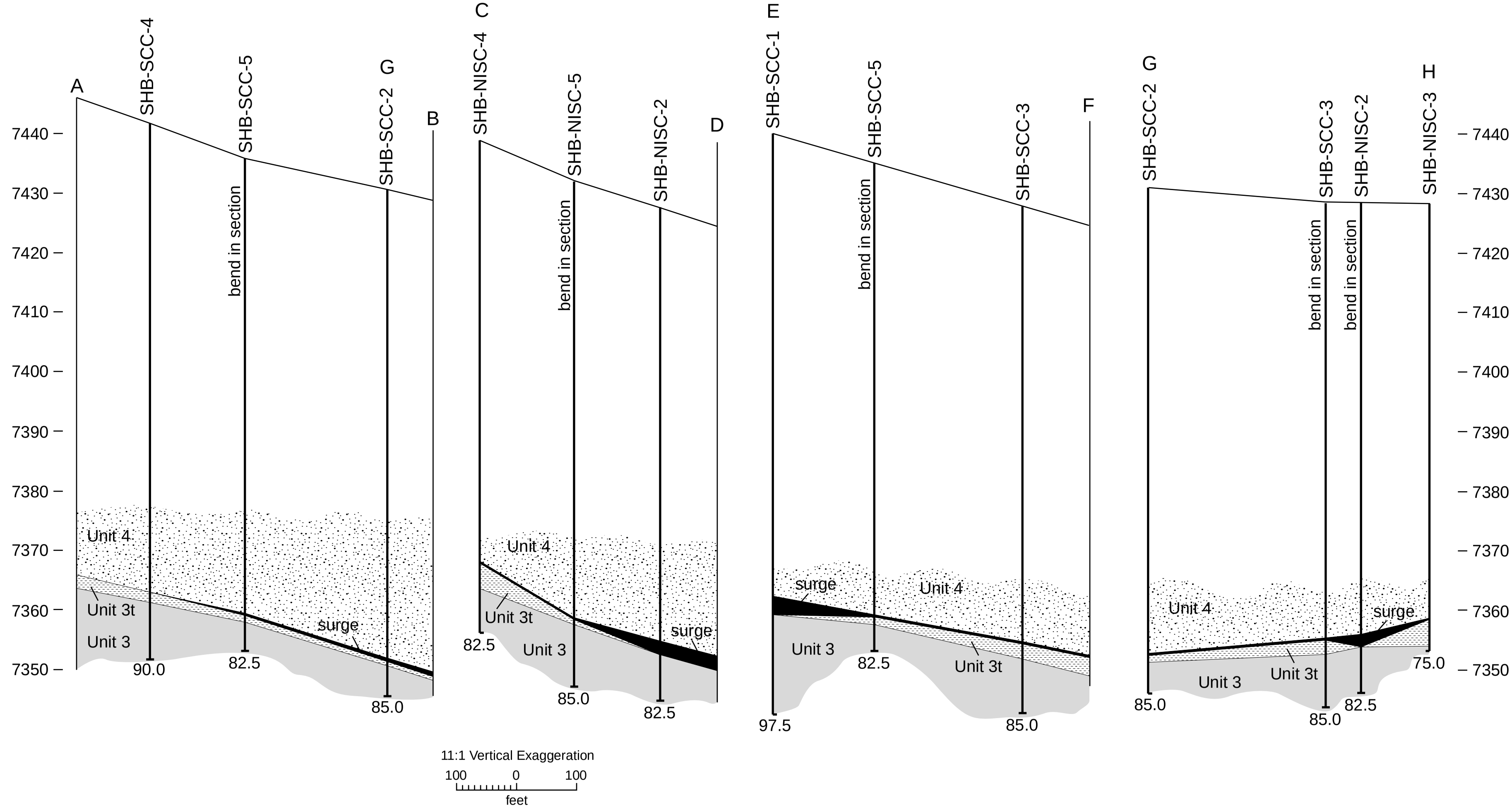

Figure 10. Cross sections AGB, CD, EF, and GH. Depths and elevations are given in feet.

and program management. Technical review was provided by David Broxton (EES). Thanks go to Anthony Garcia and Alexis Lavine for illustrations and Lanny Piotrowski for illustrations and compositing.

X. REFERENCES

Broxton, D. E., and Reneau, S. L, 1995, Stratigraphic nomenclature of the Bandelier Tuff for the Environmental Restoration Project at Los Alamos National Laboratory; Los Alamos National Laboratory report LA-13010-MS.

Chavez-Grieves Consulting Engineers, Inc., Albuquerque, NM, Strategic Computing Facility (SCC) engineering drawings, Project ID 18168, 27 April 1998.

Criss, J., 1980, Fundamental parameters calculations on a laboratory microcomputer, Advances in X-Ray Analysis **23**, pp. 93-97.

Dransfield, B.J., and Gardner, J.N., 1985, Subsurface geology of the Pajarito Plateau, Espanola Basin, New Mexico; Los Alamos National Laboratory report LA-10455-MS.

Gardner, J.N., Goff, F., Garcia, S., and Hagan, R.C.,1986, Stratigraphic relations and lithologic variations in the Jemez volcanic field, New Mexico; Journal of Geophysical Research **91**, pp. 1763-1778.

Gardner, J.N., 1998, Preliminary results from study of 1947 air photos; February 13, 1998, memo to L. Goen and D. Volkman, 2 p. plus map.

Gardner, J.N., and Goff, F., 1984, Potassium-argon dates from the Jemez volcanic field: Implications for tectonic activity in the north-central Rio Grande rift; New Mexico Geological Society Guidebook **35**, pp. 75-81.

Gardner, J.N., Lavine, A., Vaniman, D., and WoldeGabriel, G., 1998, High-precision mapping to evaluate the potential for seismic surface rupture at TA-55, Los Alamos National Laboratory; Los Alamos National Laboratory report LA-13456-MS.

Gardner, J.N., and House, L., 1987, Seismic hazards investigations at Los Alamos National Laboratory, 1984 to 1985; Los Alamos National Laboratory report LA-11072-MS.

Geological Society of America, 1980, Rock-Color Chart; Geological Society of America, Boulder, Colorado.

Goff, S., 1986, Curatorial policy guidelines and procedures for the Continental Scientific Drilling Program; Los Alamos National Laboratory report LA-10542-OBES.

Griggs, R.L., 1964, Geology and groundwater resources of the Los Alamos area, New Mexico; U.S. Geological Survey Water-Supply Paper 1753, 107 p.

Heiken, G., Goff, F., Stix, J., Tamanyu, S., Shafiqullah, M., Garcia, S., and Hagan, R., 1986, Intracaldera volcanic activity, Toledo caldera and embayment, Jemez Mountains, New Mexico, Journal of Geophysical Research **91**, pp. 1799-1815.

Izett, G.A., and Obradovich, J.D., 1994, $^{40}Ar/^{39}Ar$-age constraints for the Jaramillo Normal Subchron and the Matuyama-Brunhes geomagnetic boundary; Journal of Geophysical Research **99**, pp. 2925-2934.

Lavine, A., Heiken, G.H., and Stix, J., 1997, Stratigraphy and distribution of Cerro Toledo tephras and volcaniclastic sediments beneath the Pajarito Plateau, Jemez Mountains, New Mexico (abst.); New Mexico Geology **19**.

Olig, S., Youngs, R., and Wong, I., 1998, Preliminary probabilistic seismic hazard analysis for surface fault displacement at TA-3, Los Alamos National Laboratory; Woodward-Clyde Federal Services.

Smith, R.L., and Bailey, R.A.,1966, The Bandelier Tuff: a study of ash-flow eruption cycles and zoned magma chambers; Bulletin of Volcanology **29**, pp. 83-104.

Smith, R.L., Bailey, R.A., and Ross, C.S., 1970, Geologic map of the Jemez Mountains, New Mexico, U.S. Geological Survey Miscellaneous Geological Investigations Map I-571, 1:125,000 scale.

Stimac, J.A., Broxton, D.E., Kluk, E.C., and Chipera, S.J., Preliminary stratigraphy of tuffs from borehole 49-2-700-1 at Technical Area 49, Los Alamos National Laboratory, New Mexico (in preparation).

Warren, R.G., McDonald, E.V., and Ryti, R.T.,1998, Baseline geochemistry of soil and bedrock, Tshirege Member of the Bandelier Tuff at MDA P, Los Alamos National Laboratory report LA-13330-MS.

Wong, I., Kelson, K., Olig, S., Kolbe, T., Hemphill-Haley, M., Bott, J., Green, R., Kanakari, H., Sawyer, J., Silva, W., Stark, C., Haraden, C., Fenton, C., Unruh, J., Gardner, J., Reneau, S., and House, L., 1995, Seismic hazards evaluation of the Los Alamos National Laboratory; unpublished consulting report prepared for Los Alamos National Laboratory by Woodward-Clyde Federal Services, Oakland, California.

This report has been reproduced directly from the
best available copy.

It is available to DOE and DOE contractors from
the Office of Scientific and Technical Information,
P.O. Box 62,
Oak Ridge, TN 37831.
Prices are available from
(615) 576-8401.

It is available to the public from the
National Technical Information Service,
US Department of Commerce,
5285 Port Royal Rd.,
Springfield, VA 22616.

Los Alamos
NATIONAL LABORATORY
Los Alamos, New Mexico 87545